JOURNAL OF GEOPHYSICAL RESEARCH, VOL. 105, NO. D9, PAGES 11,617–11,623, MAY 16, 2000

Potential importance of the reaction CO + HNO_3

D. J. Lary[1]

Department of Geophysics and Planetary Sciences, Tel Aviv University, Tel Aviv, Israel

D. E. Shallcross[2]

Centre for Atmospheric Science, Cambridge University, Cambridge, England.

Abstract. CO has a strong thermodynamic potential for reducing HNO_3 to HONO. If the reaction of HNO_3 with CO does proceed via heterogeneous catalysis on sulfuric acid aerosols in our atmosphere, then this data assimilation study shows that the model is better able to reproduce the observed NO_x/HNO_3 ratio even with a γ value as low as $1x10^{-4}$. This is particularly true in the upper troposphere and lower stratosphere. We would like to highlight the possibility that elements such as iron deposited in the lower stratosphere by meteorites may be catalyzing this and other reactions within sulfate aerosols.

1. Introduction

Over just the last 5 years many studies have highlighted the fact that models do not reproduce the observed nitrogen partitioning well, and in particular the NO_x/HNO_3 ratio [*Osterman et al.*, 1999, *Singh et al.*, 1998, *Jaeglé et al.*, 1998, *Sen et al.*, 1998, *Wang and Jacob*, 1998, *Kotamarthi et al.*, 1997, *Kondo et al.*, 1997 , *Hauglustaine et al.*, 1996. *Jacob et al.*, 1996, *Folkins et al.*, 1995]. The recent World Meteorological Organization (WMO) report [*World Meteorological Organization*, 1998] concludes that below 30 km the observed NO_2/NO and NO_2/HNO_3 ratios are generally greater than usually calculated by models. Below 30 km is where we have appreciable amounts of sulfate and other types of aerosol. It is therefore well worth investigating possible candidates for surface reactions not currently considered by models.

The inability of the models to reproduce the observed NO_x/HNO_3 ratio is due to either an overestimate in the rate of HNO_3 production, an underestimate of the rate of HNO_3 destruction, or the complete omission of an HNO_3 destruction process such as an unrecognized heterogeneous reaction. A recent study [*Fairbrother et al.*, 1997] noted that CH_4 and CO have exceedingly large thermodynamic potentials for reducing HNO_3 to HONO. So it is thermodynamically feasible that the reaction of HNO_3 with CO will proceed via heterogeneous catalysis in our atmosphere [*Fairbrother et al.*, 1997]. This paper examines the likely impact of this reaction on the chemistry of the upper troposphere and stratosphere. If it does take place, then this reaction is likely to be important, as CO and HNO_3 are both species which are relatively abundant.

Even though thermodynamically feasible, it may well be that the CO + HNO_3 reaction requires a catalyst to proceed. This could be supplied by the large range of chemical elements, including iron, which are deposited in the atmosphere by ablating meteorites. Recently [*Murphy et al.*, 1998] have reported in situ measurements of meteoritic material, mercury, and other elements in aerosols in the height range 5 to 19 km.

Recent measurements [*Murphy et al.*, 1998] reveal that although stratospheric aerosols primarily consisted of sulfuric acid and water, many also contained meteoritic material. More than half of the spectra taken indicated that iron was present in the sulfate aerosols [*Murphy et al.*, 1998]. Just above the tropopause, small amounts of mercury were found in over half of the aerosol particles that were analyzed. Overall, there was tremendous variety in aerosol composition. One measure of this diversity is that at least 45 elements were detected in aerosol particles.

We would like to highlight the possibility that elements such as iron deposited in the lower stratosphere by meteorites may be catalyzing reactions within sulfate aerosols.

2. Calculations

We used the technique of four-dimensional variational (4D-VAR) data assimilation [*Fisher and Lary*, 1995] on data from the Atmospheric Trace Molecule Spectroscopy (ATMOS) Experiment to determine an optimum set of initial conditions for our numerical model calculations. This was done so that we could simultaneously use all the observations made by ATMOS,

[1] Also at the Centre for Atmospheric Science, Cambridge University, Cambridge, England.

[2] Now at the School of Chemistry, University of Bristol, Bristol, England.

Paper number 1999JD900790.
0148-0227/00/1999JD900790$09.00

together with our numerical model, to give us the best fit model simulation to these ATMOS data. Data assimilation has been used extensively in meteorology and more recently for atmospheric chemistry [*Menke*, 1984, *Courtier and Talagrand*, 1987, *Cohn*, 1997, *Courtier et al.*, 1993, *Khattatov et al.*, 1999, *Lary*, 1999, *Lary and Shallcross*, 1999]

In this study the 4D-VAR data assimilation was performed using a set of 29 stacked, independent, boxes. The boxes were stacked in the equivalent potential vorticity (PV) latitude - theta flow tracking coordinate system [*Lary et al.*, 1995] at an equivalent PV latitude of 40°S on 29 isentropic surfaces between 300 and 1800 K. The equivalent PV latitude of 40°S was chosen as we used data from the STS45/ATLAS 1 mission which was launched on March 24, 1992, from the Kennedy Space Center. During its 8 days of operation, the ATMOS instrument made observations spanning a substantial portion of the globe. The 53 measurements taken at orbital sunrise covered the midlatitude and equatorial regions of the Earth from 30°S to 30°N. The 41 sunset observations were made at 25°S to 55°S. For the duration of ATLAS 1 the equivalent PV latitude for which the vertical profiles covered the largest range of altitudes, and for which the largest number of species was observed, was centered on about 40°S. The assimilation window used was one day so that we can have 1 complete diurnal cycle.

The numerical model used is the extensively validated AutoChem model [*Fisher and Lary*, 1995]. The model is explicit and uses the adaptive timestep, error monitoring [*Stoer and Bulirsch*, 1980], time integration scheme [*Press et al.*, 1992] for stiff systems of equations. Photolysis rates are calculated using full spherical geometry and multiple scattering [*Lary and Pyle*, 1991a, *Lary and Pyle*, 1991b, *Meier et al.*, 1982, *Nicolet et al.*, 1982] with a treatment of spherical geometry [*Anderson*, 1983].

In this study the model described a total of 59 species. There were 54 integrated species are integrated, namely; $O(^1D)$, $O(^3P)$, O_3, N, NO, NO_2, NO_3, N_2O_5, HONO, HNO_3, HO_2NO_2, CN, NCO, HCN, Cl, Cl_2, ClO, ClOO, OClO, Cl_2O_2, $ClNO_2$, $ClONO_2$, HCl, HOCl, CH_3OCl, Br, Br_2, BrO, $BrONO_2$, BrONO, HBr, HOBr, BrCl, H_2, H, OH, HO_2, H_2O_2, CH_3, CH_3O, CH_3O_2, CH_3OH, CH_3OOH, CH_3ONO_2, $CH_3O_2NO_2$, HCO, HCHO, CH_4, CH_3Br, CF_2Cl_2, CO, N_2O, CO_2, and H_2O. The model contains a total of 366 reactions, 241 bimolecular reactions, 31 trimolecular reactions, 48 photolysis reactions, 46 heterogeneous reactions based on standard kinetic reference data [*DeMore et al.*, 1997, *Atkinson et al.*, 1997], with some very recent updates for NO_2 and HNO_3 kinetics [*Donahue et al.*, 1997, *Fulle et al.*, 1998, *Brown et al.*, 1999a, *Brown et al.*, 1999b].

2.1. ATMOS Case Study

Here we use 4D-VAR data assimilation to look at a case study using data from the Atmospheric Trace Molecule Spectroscopy (ATMOS) experiment to examine the effect of the postulated heterogeneous reaction CO + HNO_3. ATMOS [*Rinsland et al.*, 1996, *Abrams et al.*, 1996a, *Abrams et al.*, 1996b, *Abrams et al.*, 1996c, *Abrams et al.*, 1996d, *Abrams et al.*, 1996e, *Abbas et al.*, 1996b, *Rinsland et al.*, 1998a, *Rinsland et al.*, 1998b] is an infrared Fourier transform interferometer which has on four occasions flown in the payload bay of the space shuttle and measures the concentrations of gases present in the atmosphere at altitudes between 10 and 150 km. As the shuttle's orbit carries it into and out of the Earth's shadow, the ATMOS instrument views the Sun as it sets or rises through the atmosphere. The spectrometer measures changes in the infrared component of sunlight as the Sun's rays pass through the atmosphere. Trace gases absorb very specific wavelengths which allows the determination of which gases are present, their concentrations, and at what altitudes. ATMOS has flown four times and ATMOS. (More information on ATMOS can be found from the web site http://remus.jpl.nasa.gov/.)

2.2. NO_x/HNO_3 Ratio

The solid curve in Figure 1 shows the NO_x/HNO_3 ratio produced by performing 4D-VAR on the ATMOS data when the reaction of CO with HNO_3 on sulfate aerosols was not included in the model. The dashed line denotes

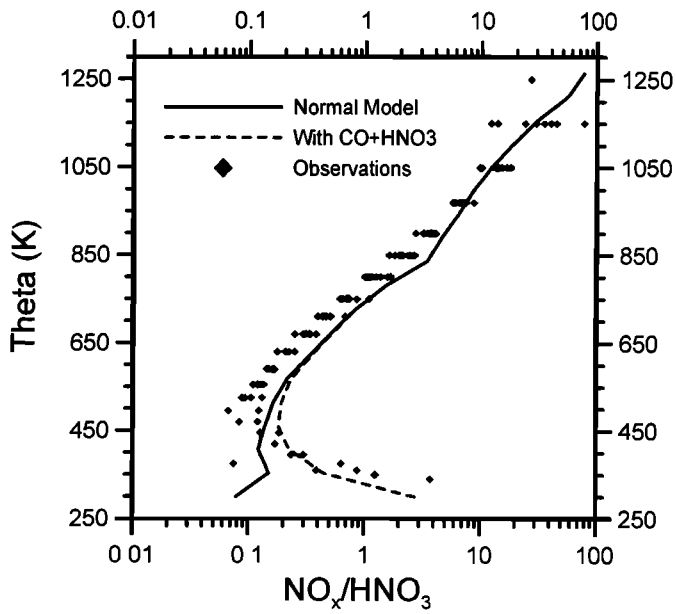

Figure 1. A comparison between the observed NO_x/HNO_3 ratio (diamonds) and that produced by performing 4D-VAR on the ATMOS data. The solid line denotes the case when the reaction of CO with HNO_3 on sulfate aerosols was not included in the model, the dashed line denotes the case when it was included in the model with γ=2x10^{-4}. The ATMOS data used simultaneously by our 4D-VAR analysis were O_3, NO, NO_2, N_2O_5, $HONO_2$, HO_2NO_2, HCN, $ClONO_2$, HCl, CH_4, CO, N_2O, CO_2, and H_2O. The vertical profile of sulfate aerosol surface area used came from the Stratospheric Aerosol and Gas Experiment 2 (SAGE 2). The observations were made by the space-shuttle-born Atmospheric Trace Molecule Spectroscopy (ATMOS) instrument on March 29, 1992.

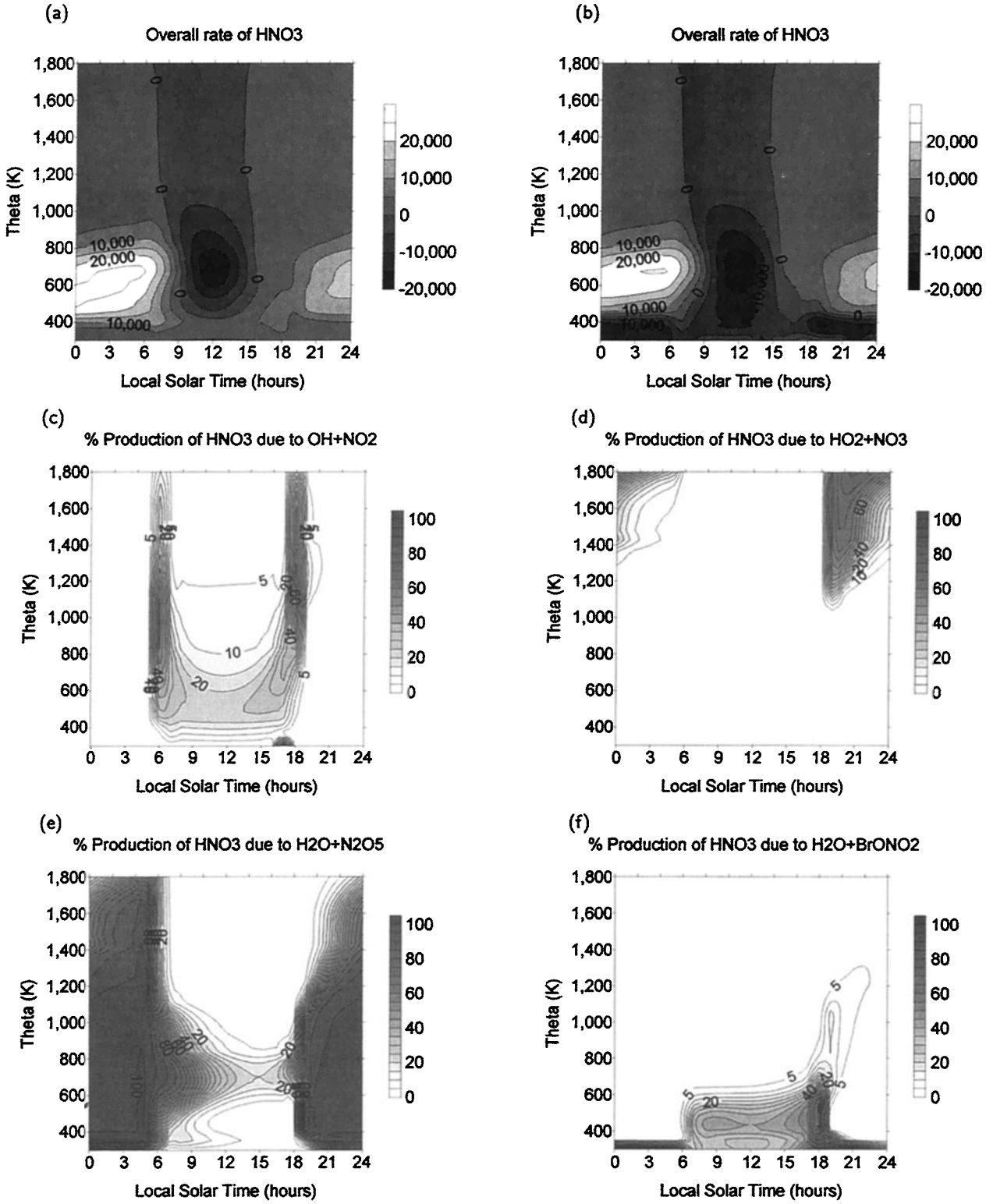

Figure 2. (a and b) Calculated net rate of change for HNO_3, in units of molecules cm^{-3} s^{-1}. Figure 2a is the calculation made without the postulated reaction of HNO_3 with CO on sulfate aerosols. Figure 2b is the calculation made with the postulated reaction with $\gamma=2x10^{-4}$. (c-f) Calculations made without the postulated reaction of HNO_3 with CO on sulfate aerosols. Figure 2c shows the calculated percentage of HNO_3 production due to the gas phase reaction of OH with NO_2. Figure 2d shows the calculated percentage of HNO_3 production due to the gas phase reaction of HO_2 with NO_3. Figure 2e shows the calculated percentage of HNO_3 production due to the hydrolysis of N_2O_5 on sulfate aerosols. Figure 2f shows the calculated percentage of HNO_3 production due to the hydrolysis of $BrONO_2$ on sulfate aerosols. In each case the x axis is local solar time in hours, and the y axis is altitude shown as a potential temperature (Kelvin).

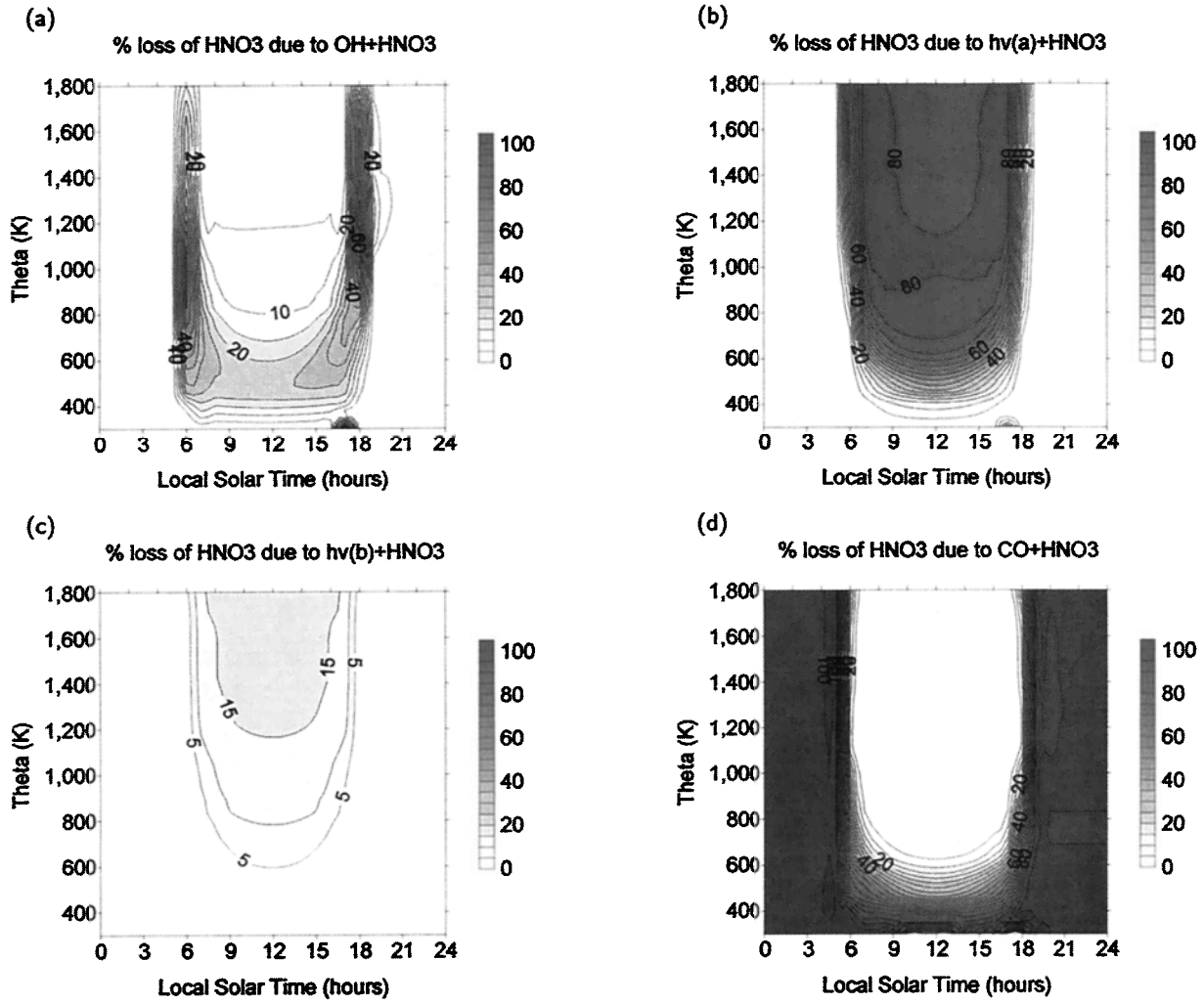

Figure 3. (a to d) are all for calculations made with the postulated reaction of HNO_3 with CO on sulfate aerosols with γ=2x10^{-4}. (a) Calculated percentage of HNO_3 destruction due to the gas phase reaction of OH with HNO_3. (b) Calculated percentage of HNO_3 destruction due to photolysis yielding OH + NO_2. (c) Calculated percentage of HNO_3 destruction due to photolysis yielding $O(^3P)$ + HONO. (d) Calculated percentage of HNO_3 destruction due to the postulated heterogeneous reaction of CO with HNO_3 with γ=2x10^{-4}. In each case the x axis is local solar time in hours, and the y axis is altitude shown as a potential temperature (Kelvin).

the case when it was included in the data assimilation with γ=2x10^{-4}.

Several values were used and γ=2x10^{-4} seemed to give the best agreement. The ATMOS data used simultaneously by our 4D-VAR analysis were O_3, NO, NO_2, N_2O_5, HNO_3, HO_2NO_2, HCN, $ClONO_2$, HCl, CH_4, CO, N_2O, CO_2, and H_2O. The vertical profile of sulfate aerosol surface area used came from the Stratospheric Aerosol and Gas Experiment 2 (SAGE 2). The diamonds are the observations of the NO_x/HNO_3 ratio made by the space shuttle born Atmospheric Trace Molecule Spectroscopy (ATMOS) instrument for March 29, 1992.

We can see in Figure 1 that even with such low values for γ the model calculations agree pretty well with the observations made by ATMOS in the lower stratosphere. Let us now examine the reason for this by looking at the chemical budget of HNO_3 calculated by the model.

2.3. Production of HNO_3

Let us look at the main production processes for HNO_3, examine their relative roles, and see how this is altered by including the postulated heterogeneous reaction CO+HNO_3 with γ=2x10^{-4}.

The most rapid HNO_3 production is in the nighttime lower stratosphere/upper troposphere. This is due to heterogeneous reactions, primarily the hydrolysis of N_2O_5 but also of $BrONO_2$ and $ClONO_2$. During the day there is a net loss of HNO_3 due to photolysis. When we add an additional loss of HNO_3, that is with the postulated reaction, the net production rate of HNO_3 during the night decreases from approximately 3.5x10^4 molecules cm^{-3} s^{-1} to 2.5x10^4 molecules cm^{-3}

s^{-1}. Figures 2a and 2b show the calculated net rates of change for HNO_3 in units of molecules cm^{-3} s^{-1} without and with the postulated reaction.

If we consider the relative contribution of the four major HNO_3 production reactions shown in Figure 2c-2f, we see that during the day the reaction of OH with NO_2 is the major source of HNO_3, particularly where there is less sulfate aerosol. During the night in the upper stratosphere the reaction of HO_2 with NO_3 may also play a role if there is a channel producing HNO_3. The reactions of NO_3 with CH_3OH and HCHO also play a small part in the nighttime upper stratosphere.

In the upper troposphere and lower stratosphere the main production of HNO_3 is due to heterogeneous reactions on sulfate aerosols (Figure 2e and 2f). The most important of these is the hydrolysis of N_2O_5. The hydrolysis of N_2O_5 makes the largest relative contribution to HNO_3 production during the night when no photolysis is occurring, and during the early morning when the N_2O_5 concentration is still relatively large (Figure 2e). But it is also interesting to see how important the hydrolysis of $BrONO_2$ is (Figure 2f), particularly as the total atmospheric loading of bromine is so much less than that of nitrogen and chlorine. The hydrolysis of $BrONO_2$ makes the largest contribution to HNO_3 production just after sunset. However, during the day between approximately 20% and 40% of the HNO_3 production is due to the hydrolysis of $BrONO_2$. The hydrolysis of $ClONO_2$ plays a minor role, peaking at about 6% just after sunset in the lower stratosphere.

2.4. Destruction of HNO_3

For most of the sunlit atmosphere the major loss is the photolysis channel which produces OH + NO_2. There is also a minor channel which produces $O(^3P)$ + HONO. However, in the lower stratosphere and upper troposphere the reaction with OH is important. Its largest relative contribution is close to sunrise and sunset Figure 3a-3c.

The contribution due to the postulated reaction of HNO_3 with CO is most important in the upper troposphere and lower stratosphere where we have the most aerosol (Figure 3d). It is also the only major nighttime loss.

2.5. Recent Gas Phase Kinetics Update

Since the last atmospheric chemistry kinetic reviews [*DeMore et al.*, 1997, *Atkinson et al.*, 1997], there have been new kinetic measurements of key reactions relevant to HNO_3 destruction and production [*Donahue et al.*, 1997, *Fulle et al.*, 1998, *Brown et al.*, 1999a, *Portmann et al.*, 1999, *Brown et al.*, 1999b]. The effects of this new kinetic data has been evaluated [*Lary and Shallcross*, 1999] who found that as the partitioning of OH and HO_2 is a strong function of the amount of NO present increasing the NO_x/HNO_3 ratio shifts the OH/HO_2 ratio in favor of OH. This increases the OH concentration by up to 40% below in the lowermost stratosphere and upper troposphere. Corresponding to this there is also a 5% to 10% increase in HCl due to the reaction of OH with ClO. The the technique of 4D-Var was used to show objectively that the new kinetic measurements result in an improvement of the model simulations [*Lary and Shallcross*, 1999]. We used these data here and recommend their use in atmospheric modeling studies.

2.6. H_2O_2 + HNO_3

It has also been noted that the reaction of H_2O_2 + HNO_3 is thermodynamically favorable [*Fairbrother et al.*, 1997]. We included this reaction in some model calculations and found that it was not likely to be a major loss of HNO_3 even with γ values of up to $2x10^{-3}$.

3. Summary

It has been noted that CO has an exceedingly strong thermodynamic potential for reducing HNO_3 to HONO [*Fairbrother et al.*, 1997]. If the reaction of HNO_3 with CO does proceed via heterogeneous catalysis in our atmosphere, then it is capable of reducing the calculated NO_x/HNO_3 ratio bringing the calculated HNO_3 profile into closer agreement with observations. Clearly measurements of this process are warranted, since a decrease of the NO_x/HNO_3 ratio leads to an increase in the oxidizing capacity of the atmosphere.

Acknowledgments. It is a pleasure to acknowledge the following: The government of Israel for an Alon Fellowship, the Royal Society for a Royal Society University Research Fellowship; the NERC and EU for research support; and Simon Hall of Cambridge University who has provided such excellent computational support. Anyone interested in performing data assimilation is welcome to contact David Lary

References

Abbas, M.M., et al., The hydrogen budget of the stratosphere inferred from ATMOS measurements of water and methane, *Geophys. Res. Lett.*, *23*(17), 2405-2408, 1996.

Abbas, M.M., et al., Seasonal variations of water vapor in the lower stratosphere inferred from ATMOS/ATLAS-3 measurements of water and methane, *Geophys. Res. Lett.*, *23*(17), 2401-2404, 1996.

Abrams, M.C., et al., On the assessment and uncertainty of atmospheric trace gas burden measurements with high resolution infrared solar occultation spectra from space by the ATMOS experiment, *Geophys. Res. Lett.*, *23*(17), 2337-2340, 1996.

Abrams, M.C., A. Goldman, M.R. Gunson, C.P. Rinsland, and R. Zander, Observations of the infrared solar spectrum from space by the ATMOS experiment, *Applied Optics*, *35*(16), 2747-2751, 1996.

Abrams, M.C., M.R. Gunson, A.Y. Chang, C.P. Rinsland, and R. Zander, Remote sensing of the ⊕'s atmosphere from space with highresolution Fourier-transform spectroscopy: Development and methodology of data processing for the ATMOS experiment, *Applied Optics*, *35*(16), 2774-2786, 1996.

Abrams, M.C., et al., ATMOS/ATLAS-3 observations of long-lived tracers and descent in the antarctic vortex in november 1994, *Geophys. Res. Lett.*, *23*(17), 2341-2344, 1996.

Anderson, D.E., The troposphere-stratosphere radiation-field at twilight - A spherical model, *Planet. Space Sci.*, *31*(12), 1517-1523, 1983.

Atkinson, R., D.L. Baulch, R.A. Cox, R.F. Hampson, J.A.

Kerr, M.J. Rossi, and J. Troe, Evaluated kinetic and photochemical data for atmospheric chemistry: supplement vi. iupac subcommittee on gas kinetic data evaluation for atmospheric chemistry, *J. Phys. Chem. Ref. Data*, *26*, 1329–1499, 1997.

Brown, S.S., R.K. Talukdar, and A.R. Ravishankara, Rate constants for the reaction $OH+NO_2 \longrightarrow HNO_3+M$ under atmospheric conditions, *Chem. Phys. Lett.*, *299*(3-4), 277–284, 1999a.

Brown, S.S., R.K. Talukdar, and A.R. Ravishankara, Reconsideration of the rate constant of the reaction of hydroxyl radicals with nitric acid, *J. Phys. Chem.*, *103*(16), 3031–3037, 1999b.

Cohn, S.E., An introduction to estimation theory, *J. Met. Soc. Japan*, *75*(1B), 257–288, 1997.

Courtier, P. and O. Talagrand, Variational assimilation of meteorological observations with the adjoint vorticity equation. 2. Numerical results, *Q. J. R. Meteorol. Soc.*, *113*(478), 1329–1347, 1987.

Courtier, P., J. Derber, R. Errico, J.F. Louis, and T. Vukicevic, Important literature on the use of adjoint, variational-methods and the Kalman filter in meteorology, *Tellus A.*, *45*(5), 342–357, 1993.

DeMore, W. B., C. J. Howard, S. P. Sander, A. R. Ravishankara, D. M. Golden, C. E. Kolb, M. J. Hampson, R. F. Molina, and M. J. Kurylo, Chemical kinetics and photochemical data for use in stratospheric modeling, JPL Publ. 97-4 12, Jet Propul. Lab., Calif. Inst. of Technol., Pasadena, 1997.

Donahue, N.M., M.K. Dubev, R. Mohrschladt, K.L. Demerjian, and J.G. Anderson, High-pressure flow study of the reactions $OH+NO_x = HNO_3$: Errors in the falloff region, *J. Geophys. Res.*, *102*, 6159–6168, 1997.

Fairbrother, D.H., D.J.D. Sullivan, and H.S. Johnston, Global thermodynamic atmospheric modeling: Search for new heterogeneous reactions, *J. Phys. Chem. A*, *101*(40), 7350–7358, 1997.

Fisher, M. and D.J. Lary, Lagrangian 4-dimensional variational data assimilation of chemical-species, *Q. J. R. Meteorol. Soc.*, *121*(527 Part A), 1681–1704. 1995.

Folkins, I.A., A.J. Weinheimer, B.A. Ridley, J.G. Walega, B. Anderson, J.E. Collins, G. Sachse, R.F. Pueschel, and D.R. Blake, O_3, NO_y, and NO_x/NO_y in the upper troposphere of the equatorial pacific, *J. Geophys. Res.*, *100*(D10), 20,913–20,926, 1995.

Fulle, D., H.F. Hamann, H. Hippler, and J. Troe, Temperature and pressure dependence of the addition reactions of OH to NO and to NO_2. IV Saturated laser-induced fluorescence measurements up to 1400 bar, *J. Phys. Chem. Ref. Data*, *108*, 5391 5397, 1998.

Hauglustaine, D.A., B.A. Ridley, S. Solomon, P.G. Hess, and S. Madronich, HNO_3/NO_x ratio in the remote troposphere during MLOPEX 2: Evidence for nitric acid reduction on carbonaceous aerosols?, *Geophys. Res. Lett.*, *23*(19), 2609–2612, 1996.

Jacob, D.J., B.G. Heikes, S.M. Fan, J.A. Logan, D.L. Mauzerall, J.D. Bradshaw, H.B. Singh, G.L. Gregory, R.W. Talbot, D.R. Blake, and G.W. Sachse, Origin of ozone and nox in the tropical troposphere: A photochemical analysis of aircraft observations over the south atlantic basin, *J. Geophys. Res.*, *101*(D19), 24235–24250, 1996.

Jaeglé, L., D.J. Jacob, Y. Wang, A.J. Weinheimer, B.A. Ridley, T.L. Campos, G.W. Sachse, and D.E. Hagen, Sources and chemistry of NO_x in the upper troposphere over the United States, *Geophys. Res. Lett.*, *25*(10), 1705–1708, 1998.

Khattatov, B. V., J. C. Gille, L.V. Lyjak, G. P. Brasseur, V. L. Dvortsov, A. E. Roche, and J. W. Waters, Assimilation of photochemically active species and a case analysis of UARS data, *J. Geophys. Res.*, *104*(D15), 18,715–18,737, 1999.

Kondo, Y., S. Kawakami, M. Koike. D.W. Fahey, H. Nakajima, Y. Zhao, N. Toriyama, M. Kanada, G.W. Sachse, and G.L. Gregory, Performance of an aircraft instrument for the measurement of NO_y, *J. Geophys. Res.*, *102*(D23), 28663–28671, 1997.

Kotamarthi, V.R., et al., Evidence of heterogeneous chemistry on sulfate aerosols in stratospherically influenced air masses sampled during PEMWest B, *J. Geophys. Res.*, *102*(D23), 28425–28436, 1997.

Lary, D.J., Data assimilation: A powerful tool for atmospheric chemistry, *Philos. Trans. R. Soc. Ser. A*, in press 1999.

Lary, D.J. and J.A. Pyle, Diffuse-radiation, twilight, and photochemistry: 1., *J. Atmos. Chem.*, *13*(4), 373–392, 1991a.

Lary, D.J. and J.A. Pyle, Diffuse-radiation, twilight, and photochemistry: 2., *J. Atmos. Chem.*, *13*(4), 393 406, 1991b.

Lary, D.J. and D.E. Shallcross, 4d-var data assimilation and the role of new rate coefficients in controlling the HNO_3/NO_x ratio, *J. Atmos. Chem.*, in press 1999.

Lary, D.J., M.P. Chipperfield, J.A. Pyle, W.A. Norton, and L.P. Riishojgaard, 3-dimensional tracer initialization and general diagnostics using equivalent pv latitude-potential-temperature coordinates, *Q. J. R. Meteorol. Soc.*, *121*(521 PtA), 187–210, 1995.

Meier, R.R., D.E. Anderson, and M. Nicolet, Radiation-field in the troposphere and stratosphere from 240-1000 nm 1. General-analysis, *Planet. Space Sci.*, *30*(9), 923–933, 1982.

Menke, W., *Geophysical Data Analysis: Discrete Inverse Theory*, Academic, San Diego, Calif., 1984.

Murphy, D.M., D.S. Thomson, and T.M J. Mahoney, In situ measurements of organics, meteoritic material, mercury, and other elements in aerosols at 5 to 19 kilometers, *Science*, *282*(5394), 1664–1669, 1998.

Nicolet, M., R.R. Meier, and D.E. Anderson, Radiation-field in the troposphere and stratosphere .2. Numerical-analysis, *Planet. Space Sci.*, *30*(9), 935–983, 1982.

Osterman, G.B., B Sen, G.C. Toon, R.J. Salawitch, J.J. Margitan, J.F. Blavier, D.W. Fahey, and R.S. Gao, Partitioning of NO_y species in the summer arctic stratosphere, *Geophys. Res. Lett.*, *26*(8), 1157–1160, 1999.

Portmann, R.W., S.S. Brown, T. Gierczak, , R.K. Talukdar, J.B. Burkholder, and A.R. Ravishankara, Role of nitrogen oxides in the lower stratosphere· A reevaluation based on laboratory studies, *Geophys. Res. Lett.*, *26*, 2387–2390, 1999.

Press, W.H., S.A. Teukolsky, W.T. Vetterling, and B.P. Flannery, *Numerical Recipes in Fortran - The Art of Scientific Computing*, Cambridge Univ. Press, New York, 2nd ed., 1992.

Rinsland, C.P., et al., Trends of OCS, HCN, SF_6, $CHClF_2$ in the lower stratosphere from 1985 and 1994 ATMOS experiment measurements near 30°N latitude, *Geophys. Res. Lett.*, *23*(17), 2349–2352, 1996.

Rinsland, C.P., et al., ATMOS/ATLAS-3 infrared profile measurements of trace gases in the november 1994 tropical and subtropical upper troposphere, *J. Quant. Spec. Rad. Trans.*, *60*(5), 891 901, 1998.

Rinsland, C.P., et al., ATMOS/ATLAS-3 infrared profile measurements of clouds in the tropical and subtropical upper troposphere, *J. Quant. Spec. Rad. Trans.*, *60*(5), 903–919, 1998.

Sen, B., G.C. Toon, G.B. Osterman, J.F. Blavier, J.J. Margitan, R.J. Salawitch, and G.K. Yue, Measurements of reactive nitrogen in the stratosphere, *J. Geophys. Res.*, *103*(D3), 3571–3585, 1998.

Singh, H.B., et al., Latitudinal distribution of reactive nitrogen in the free troposphere over the pacific ocean in late winter early spring, *J. Geophys. Res.*, *103*(D21), 28237–28246, 1998.

Stoer, J. and R. Bulirsch, *Introduction to Numerical Analysis*, Springer-Verlag, New York, 1980.

Wang, Y.H. and D.J. Jacob, Anthropogenic forcing on tropospheric ozone and OH since preindustrial times, *J. Geophys. Res.*, *103*(D23), 31123–31135, 1998.

WMO, Scientific assessment of ozone depletion: 1998, Technical Report 44, WMO Global Ozone Res. and Monitor. Proj., Geneva, Switzerland, 1998.

D. J. Lary, Department of Geophysics and Planetary Sciences, Tel Aviv University, 69978, Tel Aviv, Israel. (david.lary@atm.ch.cam.ac.uk)

D. E. Shallcross, School of Chemistry, University of Bristol, Bristol, England.

(Received February 15, 1999; revised July 22, 1999; accepted July 27, 1999.)